NASA/TM—2018–000000

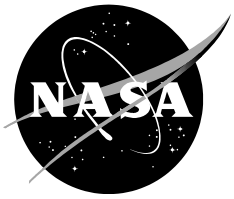

TESS Data Release Notes:
Sector 4, DR5

Michael M. Fausnaugh
Kavli Institute for Astrophysics and Space Science, Massachusetts Institute of Technology, Cambridge, Massachusetts

Christopher J. Burke
Kavli Institute for Astrophysics and Space Science, Massachusetts Institute of Technology, Cambridge, Massachusetts

Douglas A. Caldwell
SETI Institute, Mountain View, California

Jon M. Jenkins
Ames Research Center, Moffett Field, California

Jeffrey C. Smith, Joseph D. Twicken
SETI Institute, Mountain View, California

Roland Vanderspek
Kavli Institute for Astrophysics and Space Science, Massachusetts Institute of Technology, Cambridge, Massachusetts

John P. Doty
Noqsi Aerospace Ltd, Billerica, Massachusetts

Jie Li
SETI Institute, Mountain View, California

Eric B. Ting
Ames Research Center, Moffett Field, California

Joel S. Villasenor
Kavli Institute for Astrophysics and Space Science, Massachusetts Institute of Technology, Cambridge, Massachusetts

January 24, 2019

Acknowledgements

These Data Release Notes provide information on the processing and export of data from the Transiting Exoplanet Survey Satellite (TESS). The data products included in this data release are full frame images (FFIs). Due to a lapse in appropriations, the following data products for this Sector are not available at this time: target pixel files, light curve files, collateral pixel files, cotrending basis vectors (CBVs), and Data Validation (DV) reports, time series, and associated xml files

These data products were generated by the TESS Science Processing Operations Center (SPOC, Jenkins et al., 2016) at NASA Ames Research Center from data collected by the TESS instrument, which is managed by the TESS Payload Operations Center (POC) at Massachusetts Institute of Technology (MIT). The format and content of these data products are documented in the Science Data Product Description Document (SDPDD)[1]. The SPOC science algorithms are based heavily on those of the Kepler Mission science pipeline, and are described in the Kepler Data Processing Handbook (Jenkins, 2017).[2] The Data Validation algorithms are documented in Twicken et al. (2018) and Li et al. (2019). The TESS Instrument Handbook (Vanderspek et al., 2018) contains more information about the TESS instrument design, detector layout, data properties, and mission operations.

The TESS Mission is funded by NASA's Science Mission Directorate.

This report is available in electronic form at
http://https://archive.stsci.edu/tess/

[1] https://archive.stsci.edu/missions/tess/doc/EXP-TESS-ARC-ICD-TM-0014.pdf
[2] https://archive.stsci.edu/kepler/manuals/KSCI-19081-002-KDPH.pdf

1 Observations

TESS Sector 4 observations include physical orbits 15 and 16 of the spacecraft around the Earth. Two operational anomalies occurred during Sector 4—an incorrect guide star table and an instrument shutdown—and are discussed in §1.1. Data collection was paused for for 1.04 days during perigee passage while downloading data. In total, there are 22.23 days of science data collected in Sector 4.

Table 1: Sector 4 Observation times

	UTC	TJD[a]	Cadence #
Orbit 15 start	2018-10-19 09:34:28	1410.89974	132081
Guidestar tables replaced	2018-10-21 18:19:59	1413.26468	133783
Instrument anomaly start	2018-10-27 00:52:00	1418.53691	137579
Data collection resumed	2018-10-29 17:03:40	1421.21168	139505
Orbit 15 end	2018-11-01 00:11:40	1423.50890	141159
Orbit 16 start	2018-11-02 01:09:21	1424.54897	141908
Orbit 16 end	2018-11-14 08:21:39	1436.84918	150764

[a] TJD = TESS JD = JD - 2,457,000.0

The spacecraft was pointing at RA (J2000): 55.007°; Dec (J2000): −36.642°; Roll: 203.83°. Two-minute cadence data were collected for 16,000 targets, and full-frame images were collected every 30 minutes. See the TESS project Sector 4 observation page[3] for the coordinates of the spacecraft pointing and center field-of-view of each camera, as well as the detailed target list. Fields-of-view for each camera with all two-minute targets can be found at the TESS Guest Investigator Office observations status page[4].

1.1 Operations Anomalies

An incorrect guide star table was loaded into the DHU at the beginning of Sector 4. The impact on spacecraft stability was negligible, but the spacecraft pointing was offset by ∼4 arc-seconds from where it would have pointed had the correct guide star table been loaded. Thus, once the correct guide star table was loaded (TJD 1413.26), the spacecraft pointing shifted by ∼4 arc-seconds.

At TJD 1418.54, an interruption in communications between the instrument and spacecraft occurred, resulting in an instrument turn-off until TJD 1421.21. No data or telemetry were collected during this period.

1.2 Spacecraft Pointing and Momentum dumps

Sector 4 was the first set of science observations with an improved Attitude Control System (ACS) algorithm. The new ACS mode displays significantly lower pointing jitter than the

[3] https://tess.mit.edu/observations/sector-4

[4] https://heasarc.gsfc.nasa.gov/docs/tess/status.html

previous configuration—the RMS scatter of the guiding corrections are over an order of magnitude smaller than those observed for Sectors 1–3.

For the first ∼2.5 days of observations, an error in the uploaded guidestar tables resulted in a 0.5 pixel offset between the expected and commanded locations of Camera 1 and Camera 4. The ACS averages these offsets, resulting in a pointing close to the intended location; the true pointing was offset by about 4 arcseconds (∼0.2 pixels) from the commanded pointing. The guidestar tables were corrected at TJD 1421.21, removing the 4 arcsecond offset. The pointing offset and guidestar table errors did not have any effect on the pointing stability.

As in Sector 1, the reaction wheel speeds were reset to low values with momentum dumps every 2.5 days. FFIs taken during these times were marked with bit 6 (Reaction Wheel Desaturation Events). Only one or two FFIs are affected by each momentum dump.

Figure 1 summarizes the pointing performance over the course of the sector based on Fine Pointing telemetry. The ordinate axis is a factor of five smaller than in previous data releases (−1 to 1 arcsecond, rather than −5 to 5 arcseconds). The gap towards in the first half of the sector marks the instrument anomaly. The other periods of increased dispersion are generally correlated with the reaction wheels running at high speeds, and in some cases are correlated with the times of momentum dumps.

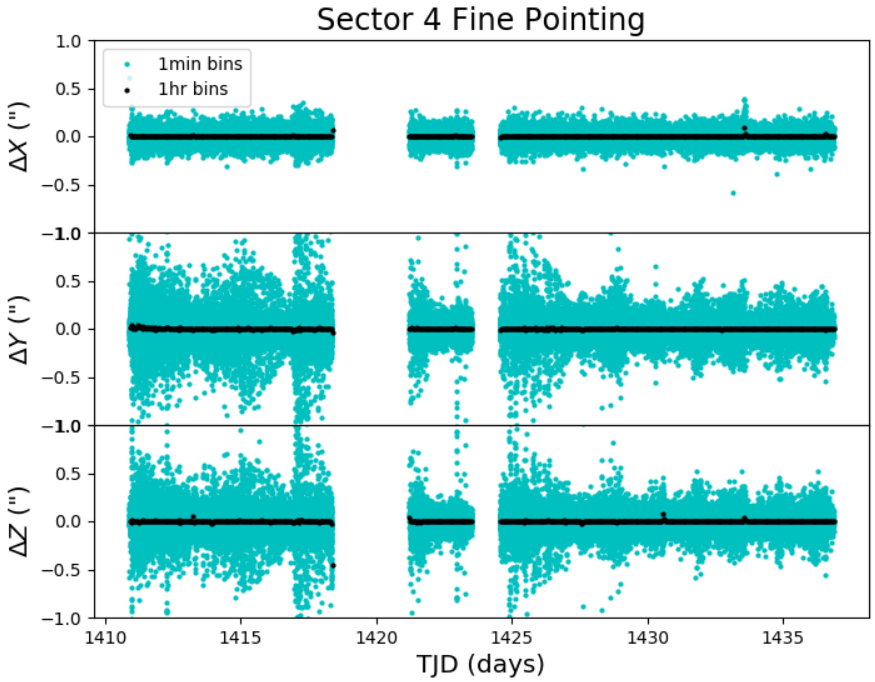

Figure 1: Guiding corrections based on spacecraft fine pointing telemetry. The delta-quaternions from each camera have been converted to spacecraft frame, binned to 1 minute and 1 hour, and averaged across cameras. Long-term trends (such as those caused by differential velocity aberration) have also been removed. The ΔX/ΔY directions represent offsets along the the detectors' rows/columns, while the ΔZ direction represents spacecraft roll. The gap towards the beginning of the observations is the instrument anomaly (see §1).

1.3 Scattered Light

Figure 2 shows the median value of the background estimate for all targets on a given CCD as a function of time. Figure 3 shows the angle between each camera's boresight and the Earth or Moon—this figure can be used to identify periods affected by scattered light and the relative contributions of the Earth and Moon to the image backgrounds. In Sector 4,the main stray light feature are caused by the Earth rising above the sunshade at the end of each orbit. The Earth reaches a minimum of 35 degrees from the center of Camera 1, and strong glints appear between TJD 1422.2297 and 1423.5020 (orbit 15) and between TJD 1436.1047 and 1436.8353 (orbit 16).

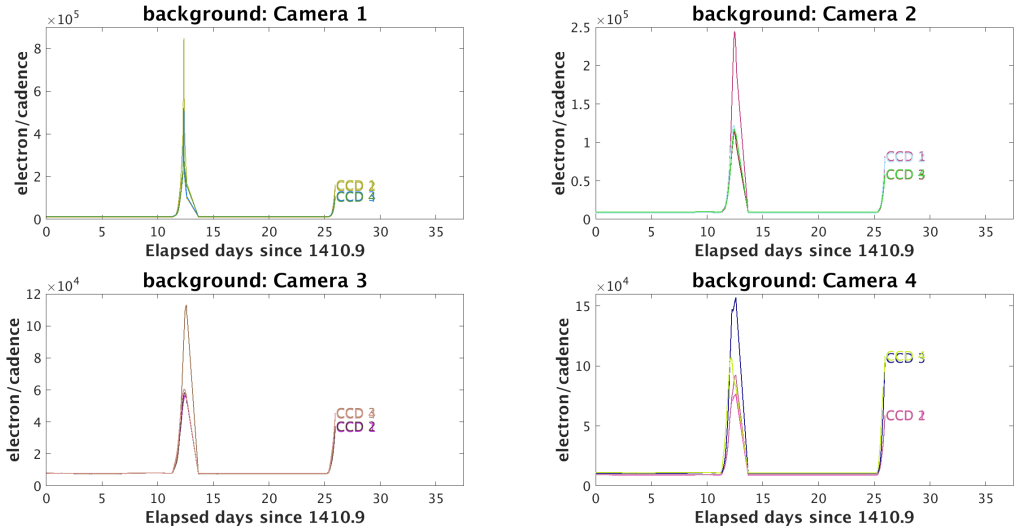

Figure 2: Median background flux across all targets on a given CCD in each camera. The changes are caused by variations in the orientation and distance of the Earth and Moon. The upturn at the end of each orbit is caused by the Earth rising above the sunshade.

2 Anomalous Effects

2.1 Smear Correction Issues

1. Camera 2, CCD 1, Column 325: There is excess charge in the virtual smear region centered on Column 459, Row 2062. The source of this effect is unclear, but the charge causes a slight over-correction of the smear in this and adjacent columns.

2. Camera 4, CCD 4, Column 1794: There is a bright star in the upper buffer rows that bleeds into the upper serial register and effects the smear rows and corresponding smear correction in this column.

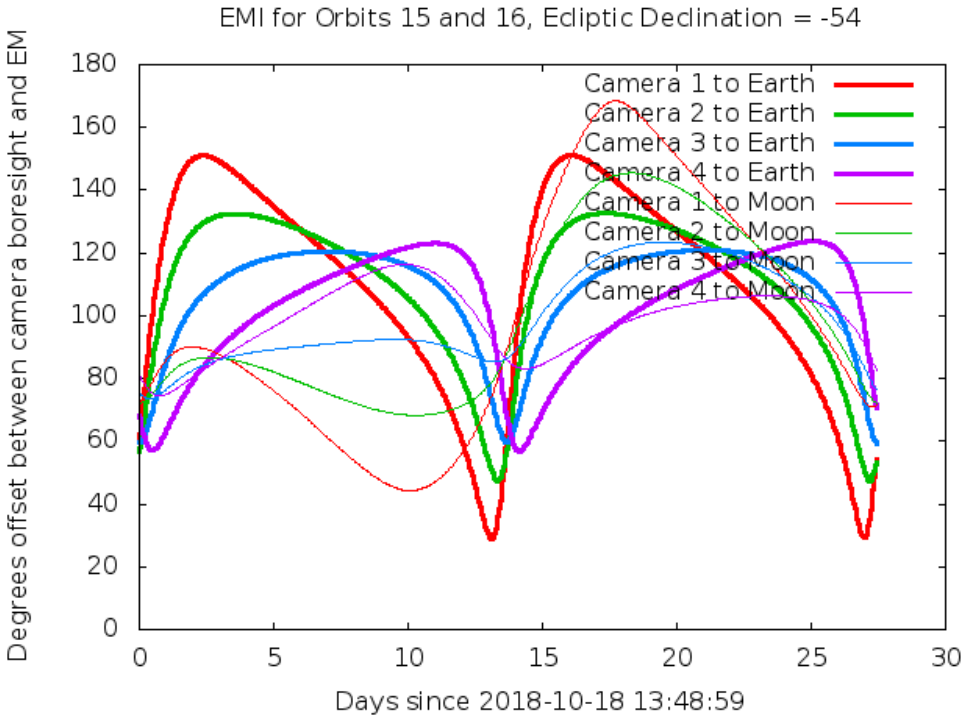

Figure 3: Angle between the four camera boresights and the Earth/Moon as a function of time. When the Earth/Moon moves within 37° of a camera's boresight, scattered light patterns and complicated features such as glints may appear. At larger angles, low level patchy features may appear. This figure can be used to identify periods affected by scattered light and the relative contributions of the Earth and Moon to the background. However, the background intensity and locations of scattered light features depend on additional factors, such as the Earth/Moon azimuth and distance from the spacecraft.

2.2 Fireflies and Fireworks

Table 2 lists all firefly and fireworks events for Sector 4. These phenomena are small, spatially extended, comet-like features in the images that may appear one or two at a time (fireflies) or in large groups (fireworks). See the instrument handbook for a complete description.

2.3 Timing Precision and Accuracy

The spacecraft clock slowly drifts relative to UTC time at a rate of a few 10s of milliseconds per day. The spacecraft clock kernel is used to correct this difference based on the measured drift rate. However, the clock kernel used to process Sector 4 data has a slight error in this measurement, resulting from extrapolation of timing measurements made during Sector 1. The reported TJD values in all data products are therefore offset by ∼1.6 seconds at the end of orbit 16 (2018-11-14 UTC). This error also implies that the durations of the FFIs are underestimated by about 280 microseconds. This issue will be corrected if the data are reprocessed in a future data release.

Table 2: Sector Fireflies and Fireworks

FFI Start	FFI End	Cameras	Description
2018293202940	2018293205940	2, 3	single firefly
2018303135940	2018303142940	1	single firefly
2018306015940	2018306022940	1, 2	single firefly
2018308055940	2018308062940	1, 2	fireflies
2018308122940	2018308125940	2	single firefly
2018309015940	2018309022940	2	single firefly
2018309225940	2018309232940	3, 4	single firefly
2018312035940	2018312042940	1, 2	fireflies
2018317142940	2018317145940	2, 3, 4	fireworks

References

Jenkins, J. M. 2017, Kepler Data Processing Handbook: Overview of the Science Operations Center, Tech. rep., NASA Ames Research Center

Jenkins, J. M., Twicken, J. D., McCauliff, S., et al. 2016, in Proc. SPIE, Vol. 9913, Software and Cyberinfrastructure for Astronomy IV, 99133E

Li, J., Tenenbaum, P., Twicken, J. D., et al. 2019, *PASP*, 131, 024506

Twicken, J. D., Catanzarite, J. H., Clarke, B. D., et al. 2018, *PASP*, 130, 064502

Vanderspek, R., Doty, J., Fausnaugh, M., & Villaseñor, J. 2018, TESS Instrument Handbook, Tech. rep., Kavli Institute for Astrophysics and Space Science, Massachusetts Institute of Technology

Acronyms and Abbreviation List

BTJD Barycentric-corrected TESS Julian Date

CAL Calibration Pipeline Module

CBV Cotrending Basis Vector

CCD Charge Coupled Device

CDPP Combined Differential Photometric Precision

COA Compute Optimal Aperture Pipeline Module

CSCI Computer Software Configuration Item

CTE Charge Transfer Efficiency

Dec Declination

DR Data Release

DV Data Validation Pipeline Module

DVA Differential Velocity Aberration

FFI Full Frame Image

FIN FFI Index Number

FITS Flexible Image Transport System

FOV Field of View

FPG Focal Plane Geometry model

KDPH Kepler Data Processing Handbook

KIH Kepler Instrument Handbook

KOI Kepler Object of Interest

MAD Median Absolute Deviation

MAP Maximum A Posteriori

MAST Mikulski Archive for Space Telescopes

MES Multiple Event Statistic

NAS NASA Advanced Supercomputing Division

PA Photometric Analysis Pipeline Module

PDC Pre-Search Data Conditioning Pipeline Module

PDC-MAP Pre-Search Data Conditioning Maximum A Posteriori algorithm

PDC-msMAP Pre-Search Data Conditioning Multiscale Maximum A Posteriori algorithm

PDF Portable Document Format

POC Payload Operations Center

POU Propagation of Uncertainties

ppm Parts-per-million

PRF Pixel Response Function

RA Right Ascension

RMS Root Mean Square

SAP Simple Aperture Photometry

SDPDD Science Data Product Description Document

SNR Signal-to-Noise Ratio

SPOC Science Processing Operations Center

SVD Singular Value Decomposition

TCE Threshold Crossing Event

TESS Transiting Exoplanet Survey Satellite

TIC TESS Input Catalog

TIH TESS Instrument Handbook

TJD TESS Julian Date

TOI TESS Object of Interest

TPS Transiting Planet Search Pipeline Module

UTC Coordinated Universal Time

XML Extensible Markup Language